

ORIGINAL RESEARCH

Simultaneous growth of two cancer cell lines

Hamon et al

Simultaneous growth of two cancer cell lines evidences variability in growth rates

Agnès Hamon^{1,2,3}

Marie Tosolini^{3,4,5,6}

Bernard Ycart^{1,2,3}

Frédéric Pont^{3,4,5,6}

Jean-Jacques Fournié^{3,4,5,6}

¹Université Grenoble-Alpes, France

²Laboratoire Jean Kuntzmann, CNRS UMR 5224, Grenoble, France

³Laboratoire d'Excellence 'TOUCAN', France

⁴INSERM UMR1037, Cancer Research Center of Toulouse, Toulouse, France

⁵Université Toulouse III Paul-Sabatier, Toulouse, France

⁶ERL 5294 CNRS, Toulouse, France

Correspondence: Bernard Ycart

51 rue des mathématiques, 38041 Grenoble cedex, France

Tel: +33476514995

Fax: +33476631263

E-mail: bernard.ycart@imag.fr

Abstract: Cancer cells co-cultured in vitro reveal unexpected differential growth rates that classical exponential growth models cannot account for. Two non-interacting cell lines were grown in the same culture, and counts of each species were recorded at periodic times. The relative growth of population ratios was found to depend on the initial proportion, in contradiction with the traditional exponential growth model. The proposed explanation is the variability of growth rates for clones inside the same cell line. This leads to a log-quadratic growth model that provides both a theoretical explanation to the phenomenon that was observed, and a better fit to our growth data.

Keywords: cell growth; log-linear model

Introduction

Since emergence of resistant cells underlies time to relapse for cancer patients undergoing chemotherapy, the growth rate of these tumor cells is a crucial issue. Cancer therapies usually yield undetectable levels of residual and resistant cancer stem cells (CSC) in patients. Upon repeated mitosis however, CSC can seed a cell progeny that progressively reconstitutes tumors, but the proportion and mitotic rate of such CSC are highly variable in treated patients. The classical exponential growth model predicts that the relative growth of the fast-growing clones should increase exponentially with time, regardless of their initial rates in patients. On the other hand however, this model is challenged by heterogeneity of the clonal progeny from a cancer cell and the resulting Darwinian selection in this progeny for access to nutriment.^{1,2} To investigate this, we grew either separately or together, two different non-interacting human cancer cell lines, in cell cultures with unlimited medium supply, and modeled the cell growth rates observed in the co-cultures. The exponential growth model is so elementary and has been known for such a long time,^{3,4} that it seems almost too simple to actually fit real cell growth data.⁵ Yet, for a given cell line grown in unlimited supporting medium, an excellent linear fit is usually observed for the logarithm of population size against time.^{6,7} Our experiments were conducted with two well known lab strains: RL (non-Hodgkin's lymphoma B cell line: ATCC CRL-2261⁸) and THP-1 (cell line derived from an acute monocytic leukemia patient: TCC TIB-202⁹). As a control experiment, the two cell lines were grown separately. An excellent log-linear fit was observed. Then, both strains were grown in the same solution. No interaction between the two

species could occur, other than possible competition for nutrient from culture medium. This was avoided again by maintaining a sufficient supply of medium by volume, and continuous renewal. The initial proportions of the faster growing strain RL were fixed at 0.5%, 1%, 5%, and three replicates were made for each initial proportion. With the classical exponential growth model, the relative proportion of RL vs. THP-1 would be predicted to increase exponentially in time, at a rate which is independent from the initial proportion. Somewhat unexpectedly, this turned out to be false. Figure 1 presents a plot of the ratio of observed RL vs THP-1 counts on a logarithmic scale. The time scales have been shifted so that the origin corresponds to the time at which each proportion reaches 5%. The slope of the regression line decreases as the initial proportion of the faster strain increases: the slope with an initial proportion 5% (red) is smaller than that with initial proportions 1% (green) and 0.5% (blue).

In vitro experiments with simultaneous growth of two or more microorganisms have long been carried through: see Dykhuizen¹⁰ for a review. The variability of growth rates in human leukemia cell clones has been studied by Tomelleri et al.¹¹ However, to the best of our knowledge, this is the first instance describing an experiment with two different cancer lines, and showing the phenomenon of dependence of the ratio growth rate on the initial condition, illustrated on Figure 1.

The objective of this paper is to propose a stochastic growth model explaining the phenomenon, and show that the fit of the data by that model is better than with the exponential growth model.

It has long been known that exponential proliferation is a valid approximation, only on a certain fraction of the observation time.¹² Many different models have been proposed as growth curves.^{13,14} At the beginning of a cell growth experiment, a lag phase^{15,16,17} is usually observed; this is the case in our data. The lag phase could partly account for the phenomenon investigated here. Indeed, when starting from a 0.5% proportion, the lag phase has elapsed when reaching 1%, but if one already starts with a 1% proportion, the lag phase only begins. Yet the lag phase does not explain differential growth rates after all cultures have reached a 5% proportion, since at that time, the lag phase has elapsed in the first two cases. Another simple explanation is proposed here: intrinsic variability of growth rates.^{5,11} Here, the notion of growth rate is understood in the sense of branching processes,⁴ as a “large scale approximation” that applies to the whole clone stemming from a given cell, and not just to

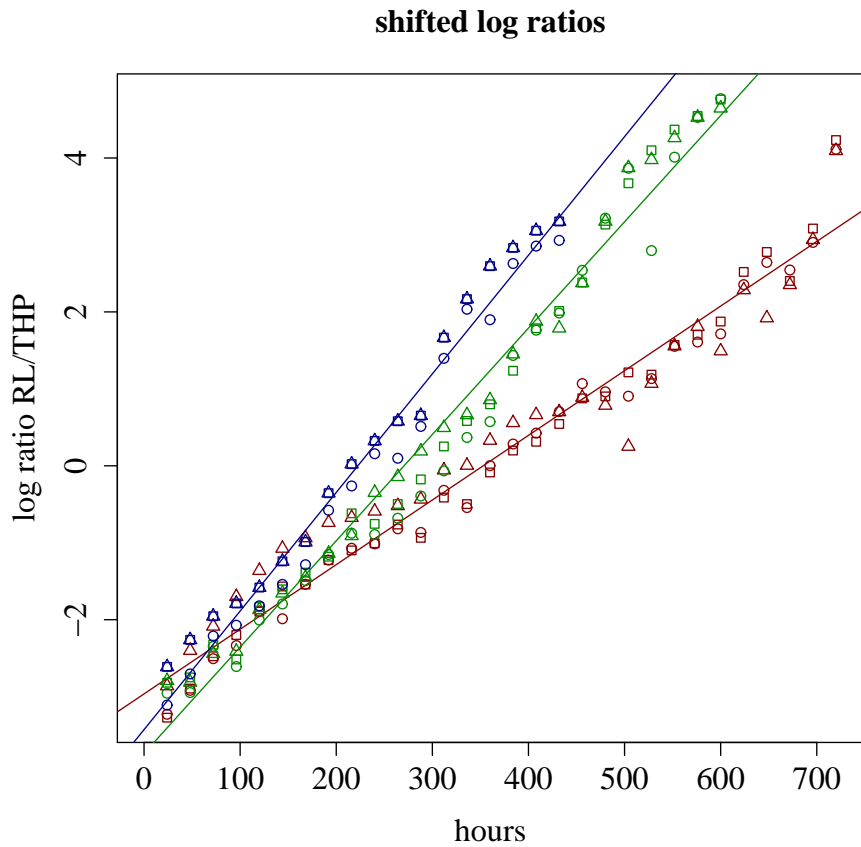


Figure 1: Logarithms of ratios of RL/THP-1. The three replicates for each initial condition are marked by circles, triangles and squares. All curves have been shifted to the first day where the proportion RL/THP-1 passes 5%. Red marks correspond to an initial proportion of 5%, green marks to 1%, blue marks to 0.5%. The three regression lines are represented with corresponding colors. The slopes (time unit: hour) are 0.0084 (red line, initial proportion 5%), 0.0138 (green line, initial proportion 1%), and 0.0154 (blue line, initial proportion 0.5%).

that cell. Therefore, the variation of growth rates can only be genetic: to each cell present at the beginning of the experiment is associated one value, which will be the growth rate of the whole clone stemming from that cell. If growth rates among RL vary, the proportion of fast dividing mitotic cells among RL cell clones will gradually increase. When reaching the proportion of 5%, there will be more fast breeders among RL if the initial proportion was 0.5%, than if it was 1%. This intuitively explains why the estimated growth rate over a given time interval, is larger when the proportion of RL reaches 5%, after starting from 0.5%.

Mathematically, it will be shown that assuming variable growth rates among the cells of a same species, naturally leads to a log-quadratic model on the population growth, instead of the traditional log-linear (or exponential) model. It will be shown that the log-quadratic model induces a better fit on our data. Using that model, the observed phenomenon can be explained and quantified. Indeed, if the actual growth is log-quadratic instead of log-linear, the fit of a log-linear model yields estimated slopes that vary with the initial condition: Figure 2 illustrates that theoretical explanation. The derivation of the log-quadratic model from the hypothesis of variable growth rates uses the cumulant generating function of the random growth rates. A similar explanation had been proposed by Hansen.¹⁸

Material and methods

Experimental methods

The cell line THP-1 (ATCC TIB-202) derives from human acute monocytic leukemia. It has a monocyte morphology and expresses the cell surface marker CD13. The cell line RL (ATCC CRL-2261) was derived from human non-Hodgkin's lymphoma and expresses the cell surface marker CD20. These two cell lines were cultured as indicated by the supplier (ATCC www.lgcstandards-atcc.org) at 37°C and 5% CO₂ in liquid medium RPMI-1640 (LONZA, Levallois, France) supplemented with 10% heat-inactivated fetal calf serum (FCS), 2mM L-glutamine, 100 U/ml penicillin and 100g/ml streptomycin (Invitrogen, Cergy Pontoise, France). This medium contains inorganic salt, amino acid, vitamins and D-glucose (2g/L). THP-1 and RL, alone and in competition, were cultured in T75 flasks with 50mL of medium without agitation. At the beginning of the culture, for all the conditions, cells were seeded at 0.3×10^6 cells/mL. Daily,

equivalent slopes on log-quadratic models

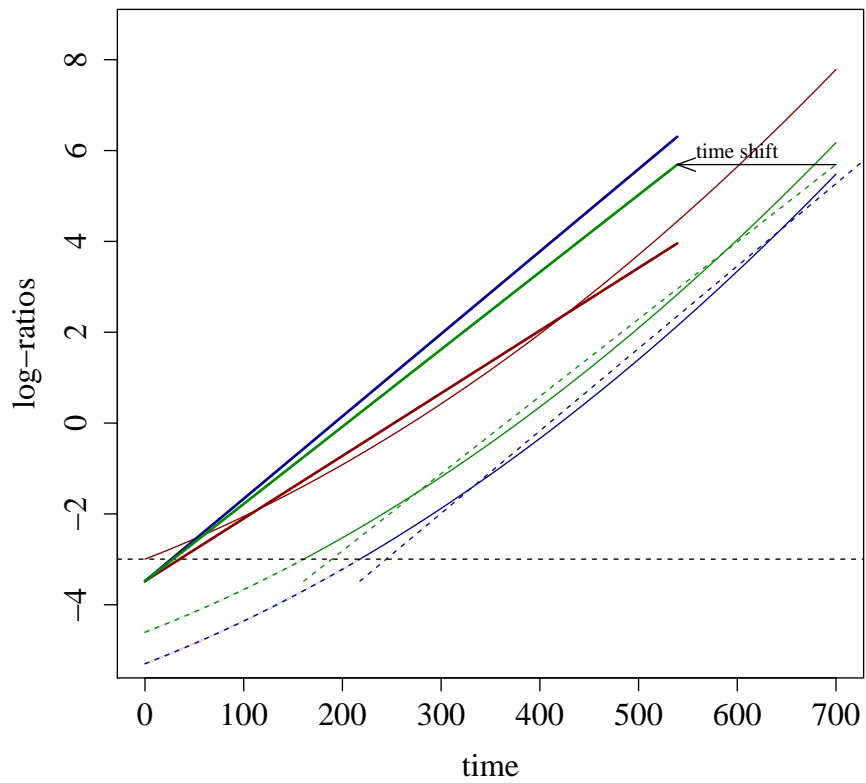


Figure 2: Theoretical explanation for observed differential growth rates. The figure represents a quadratic growth in time, at 3 different intercepts: $\log(0.05)$ (red), $\log(0.01)$ (green), $\log(0.005)$ (blue). The three solid curves are parabolas. The green and blue dashed lines are linear fits over an interval starting at the point where the corresponding parabola reaches $\log(0.05)$. The green and blue solid lines are time shifts, illustrating the differential slopes.

the different cell cultures were counted and if necessary, diluted with complete medium if the cell concentration was higher than 0.7×10^6 cells/mL to adjust at 0.3×10^6 cells/mL. These concentrations lead to no competition for nutrient. The dilutions of the culture were adjusted to the cell growth in each flask: RL cell culture was more diluted than THP-1 cell culture for example. Cells from competition cultures were also analysed by flow cytometry to determine the percentage of each cell line in the culture: Cells were centrifuged, washed with PBS and incubated 10 min with antibodies against CD20 coupled with the fluorochrome APC-Cy7 to identify RL cells, and against CD13 coupled with the fluorochrome PE (BD Biosciences, Pont de Claix, France) to identify THP-1 cells. Cells from single cell line culture were used as controls. The fluorescence of 50000 cells was then analysed using a BD LSR II cytometer.

Two sets of experiments were carried through 35 days, with daily measurements. In the first set, the two cell lines RL and THP-1 were grown in separate culture flasks, in duplicate. In the second set, the two cell lines were grown in the same culture flask, in triplicate, with unlimited amount of nutrient in each case. Three initial proportions of RL (the faster growing strain) were considered: 0.5%, 1%, and 5%. For each set of experiment, each day of culture, and each replicate, numbers of cells of each type were recorded. The dataset is available upon request. On these data, different least square fits of the log-quadratic model (6) were performed, for each of the two separate growths (first set of experiments), and for simultaneous growth (second set).

Mathematical model

In this section, a mathematical derivation of a log-quadratic growth model, based on variable growth rates, is proposed.

Consider first the classical model of exponential growth for a single clone, stemming from the general theory of branching processes.^{19,20,4} From a single cell at time 0, the clone grows to size $N(t)$ at time t . Under fairly general hypotheses on the division time distribution, there exists a positive constant b , the growth rate (also called Malthusian parameter), such that almost surely:

$$\lim_{t \rightarrow +\infty} e^{-bt} N(t) = C, \quad (1)$$

where C is a random variable with finite expectation and variance. This is one of the basic results of the theory of branching processes.^{19,20} Thus it is reasonable to assume $N(t) = Ce^{bt}$ as a model of growth curve for a single clone. Assume now that the population grows from a large number n of identical initial

cells. For $i = 1, \dots, n$, let $N_i(t)$ be the size at time t of the clone stemming from cell i :

$$N_i(t) = e^{bt} C_i, \quad (2)$$

where the C_i are independent identically distributed random variables. The total population at time t is:

$$N(t) = \sum_{i=1}^n N_i(t).$$

By the law of large numbers, almost surely:

$$\lim_{n \rightarrow \infty} \frac{N(t)}{n} = e^{vt} \mathbb{E}(C),$$

where $\mathbb{E}(C)$ denotes the mathematical expectation of the random variable C . This justifies the classical log-linear model:

$$\log(N(t)) = a + bt, \quad (3)$$

where $a = \log(N(0))$. General references on log-linear models are Mair²¹ and von Eye and Mun.²²

Consider now a second population growing according to the same model, and denote by $M(t)$ its size at time t .

$$\log(M(t)) = a' + b't.$$

Assume $b > b'$ (the first population grows faster). Then the ratio $R(t) = N(t)/M(t)$ also follows a log-linear model.

$$\log(R(t)) = (a - a') + (b - b')t.$$

Whatever the interval of time it is observed on, the growth rate $b - b'$ does not depend on the interval nor on the initial proportion. This is contradicted by our observation (Figure 1).

Assume now that clones stemming from different initial cells may have different growth rates. The new model is:

$$N_i(t) = e^{B_i t} C_i, \quad (4)$$

where (B_i, C_i) are independent and identically distributed copies of a random couple (B, C) . The joint distribution of (B, C) is of course unknown, and we shall make the technical assumptions that B and C are independent, and that

B has faster than exponential decaying tails. By the same argument of law of large numbers, the global population $N(t)$ should satisfy:

$$\log(N(t)) = a + \log(\mathbb{E}(e^{Bt})) .$$

Note that the function $\log(\mathbb{E}(e^{Bt}))$ exists for all $t \geq 0$ if the distribution of B has faster than exponential decaying tails. This function is the cumulant generating function of B ,²³ well known in large deviation theory.²⁴ Let μ be the expectation of B , σ its standard deviation and γ_1 its skewness. Then the first three terms of the Taylor expansion of $\log(\mathbb{E}(e^{Bt}))$ are:

$$\log(\mathbb{E}[e^{Bt}]) = \mu t + \frac{\sigma^2}{2} t^2 + \frac{\sigma^3 \gamma_1}{6} t^3 + o(t^3) , \quad (5)$$

In the particular case where B follows the Gaussian distribution, the first two terms give the exact expression:

$$\log(\mathbb{E}[e^{Bt}]) = \mu t + \frac{\sigma^2}{2} t^2 .$$

In that case, the growth of $N(t)$ is quadratic in logarithmic scale:

$$\log(N(t)) = a + bt + ct^2 , \quad (6)$$

with $a = \mathbb{E}[N_0]$, $b = \mu$, and $c = \sigma^2/2$. Equation (6) will be referred to as *log-quadratic model*: see Chapter 9 of von Eye and Mun,²² and Stone et al²⁵ for an application in a similar context. Assuming that the distribution of B is Gaussian may seem unrealistic, but whatever the distribution of B , if its expectation is $\mu = b$ and variance $\sigma^2 = 2c$, equation (6) remains true as a second order approximation, because of (5). This justifies the use of (6) as a model, in case of variable growth rates.

If two populations grow according to a log-quadratic model, then the ratio of the two population sizes does too. Denote again that ratio by $R(t)$, assuming that the choice has been made to put the faster growing population on the numerator, so that $R(t)$ increases.

$$\log(R(t)) = a + bt + ct^2 , \quad (7)$$

with $a = \log(R(0))$ and $b, c > 0$. In practice, growth rates are estimated by a log-linear regression over a given interval, say $[T_1, T_2]$. This amounts to approximating (7) by:

$$\log(R(t)) = \hat{\alpha} + \hat{\beta}t ,$$

where $\hat{\alpha}$ and $\hat{\beta}$ are optimal in the sense of mean squares:

$$(\hat{\alpha}, \hat{\beta}) = \arg \min \int_{T_1}^{T_2} (a + bt + ct^2 - \alpha - \beta t)^2 dt . \quad (8)$$

The solution of (8) is easily obtained:

$$\hat{\alpha} = a - \frac{c}{6}(T_1^2 + T_2^2 + 4T_1T_2) \quad \text{and} \quad \hat{\beta} = b + c(T_1 + T_2) .$$

For a fixed span $T_2 - T_1$, the “equivalent growth rate” $\hat{\beta}$ increases as T_1 increases (see Figure 2 for an illustration). This explains the phenomenon evidenced by Figure 1. More precisely, let T_1 be the time at which R reaches the value $R_1 > R(0)$:

$$T_1 = \frac{1}{2} \left(-b + \sqrt{b^2 + 4c \log \left(\frac{R_1}{R(0)} \right)} \right) .$$

The equivalent growth rate on a time interval of duration t after T_1 will be $\hat{\beta} = b + c(2T_1 + t)$. It will be larger than the growth rate on an interval of same width starting at 0, which is $b + ct$.

Thus the log-quadratic model (6) provides a theoretical explanation for the phenomenon of differential growth rates, that has been observed. As will be shown in the next section, it also provides a better fit to our data.

Results

Separate growth of RL

Let Y_{ik} denote the logarithm of cell count at time t_k and replicate i ($i = 1, 2$). We consider the following model :

$$Y_{ik} = a + bt_k + ct_k^2 + \varepsilon_{ik} , \quad (9)$$

where ε_{ik} are centered Gaussian random variables with common standard-deviation. For RL cells, it turned out that the coefficient c , that we shall call “curvature”, was not significantly different from zero ($P = 0.698$). Therefore a linear model without quadratic term was fitted. Table 1 reports the estimated coefficients. Figure 3 presents the residual analysis. The two coefficients a and b are significantly different from zero. The 95% confidence interval of the mean RL growth rate b is $[0.0311; 0.0315]$. This corresponds to a doubling time between 22 and 22.3 hours. The proportion of the variation of Y_{ik} explained by the

Coefficient	Estimate	Std. Error	P
a	12.21	3×10^{-2}	$< 2 \times 10^{-16}$
b	0.0313	9×10^{-5}	$< 2 \times 10^{-16}$

Table 1: Estimations for the logarithm of RL cell counts.

Coefficient	Estimate	Std. Error	P
a	12.37	5×10^{-2}	$< 2 \times 10^{-16}$
b	0.0212	4×10^{-4}	$< 2 \times 10^{-16}$
c	5×10^{-6}	7×10^{-7}	8.6×10^{-11}

Table 2: Estimations for the logarithm of THP-1 cell counts.

fitted model is excellent ($R^2 = 0.99$). The QQ-plot of residuals (figure 3) is close to linear, the plot of residuals vs. time does not show any mis-specification of the non-random part nor heteroscedasticity problem. The Durbin-Watson test ($P = 0.12$) and the runs test ($P = 0.69$) indicate no violation of the hypothesis of error independence.

Separate growth of THP-1

The model remains the same, see equation (9). At first, it was fitted to the full data set. Three observations at the end of the experiment period, were detected as outliers, and therefore excluded from the final analysis. Table 2 reports the estimated coefficients. Figure 4 presents the residual analysis. Contrarily to the RL case, the curvature c is significantly positive ($P = 8.6 \times 10^{-11}$). The proportion of the variation of Y_{ik} explained by the fitted model is excellent ($R^2 = 0.99$). The 95% confidence interval of the mean THP-1 growth rate b is $[0.0204; 0.0227]$. This corresponds to a doubling time between 30.5 and 34 hours, i.e. slightly below the values given in Tsuchiya et al⁹ (35 to 50 hours), and above those of Tsuchiya et al²⁶ (24 to 30 hours).

The QQ-plot of residuals (figure 4) is close to linear, the plot of residuals vs. time does not show any mis-specification of the non-random part nor heteroscedasticity problem. The Durbin-Watson test ($P = 0.16$) and the runs test ($P = 0.75$) indicate no violation of the hypothesis of error independence.

As expected, the growth rate of THP-1 is significantly smaller than that of RL ($P < 0.0001$).

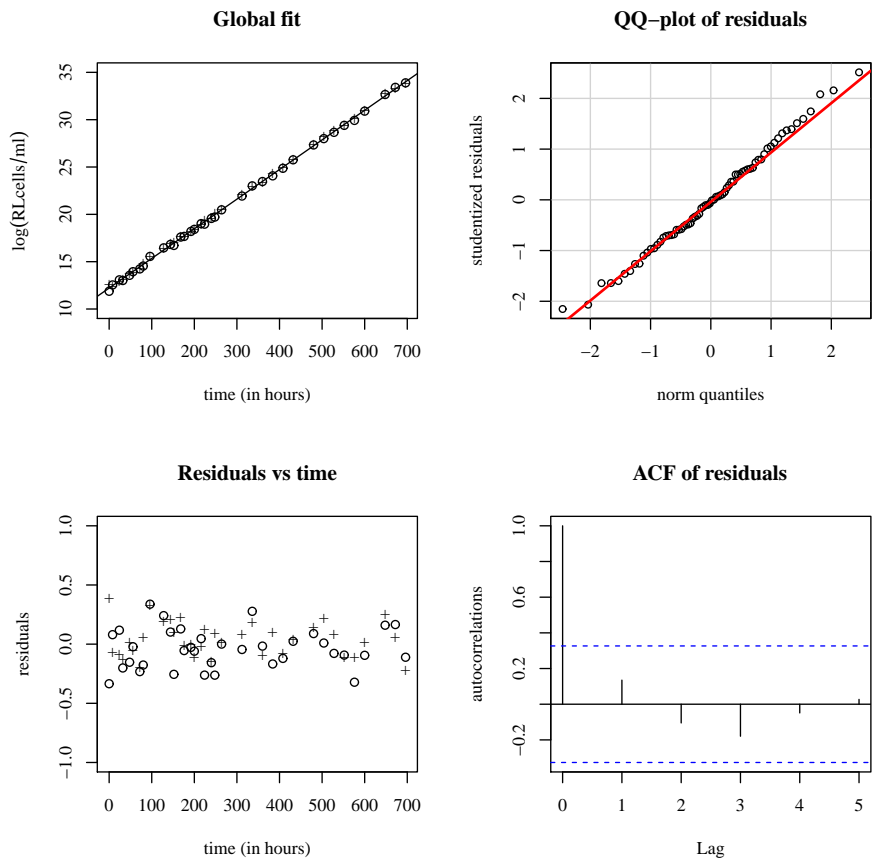


Figure 3: Fit and validation of the log-linear model: RL cells.

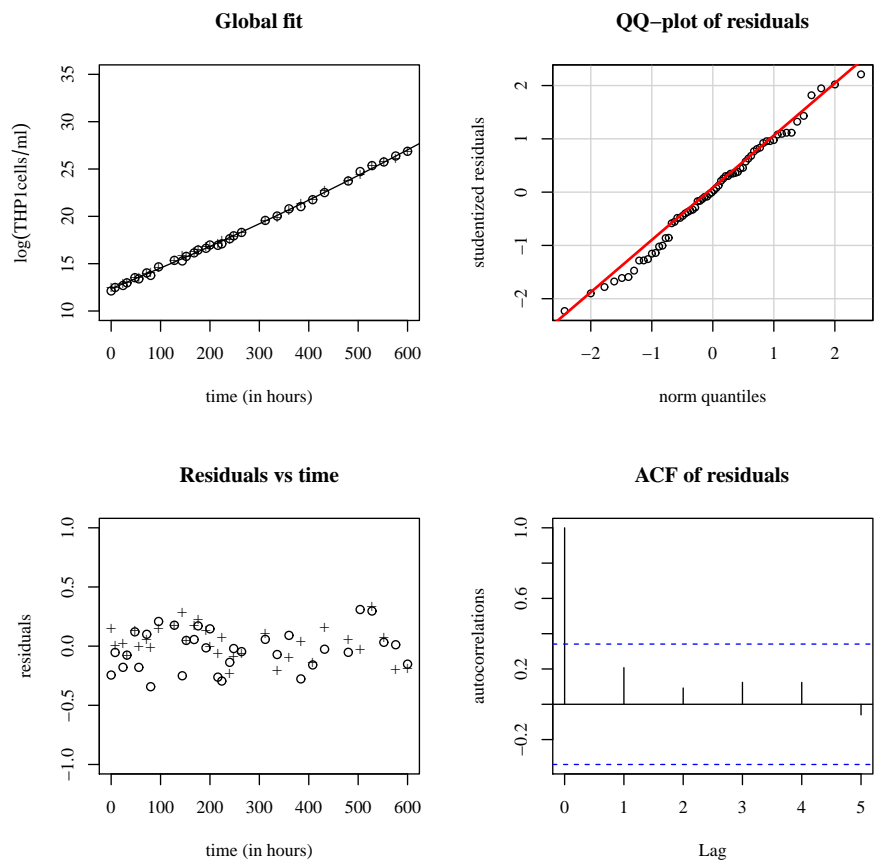


Figure 4: Fit and validation of the log-quadratic model: THP-1 cells.

Simultaneous growth of RL and THP-1

Let Y_{ijk} denote the logarithm of the ratio of RL by THP-1 cell counts at time t_k , where i denotes the replicate ($i = 1, 2, 3$) and j the initial nominal value of the ratio, that will be called *dilution*. Indices $j = 1, 2, 3$ correspond to dilutions 0.5%, 1%, 5%. Four different models were considered:

$$Y_{ijk} = a + a_j + bt_k + \epsilon_{ijk} \quad (\text{M0})$$

$$Y_{ijk} = a + a_j + bt_k + b_j t_k + \epsilon_{ijk} \quad (\text{M1})$$

$$Y_{ijk} = a + a_j + bt_k + b_j t_k + ct_k^2 + \epsilon_{ijk} \quad (\text{M2b})$$

$$Y_{ijk} = a + a_j + bt_k + ct_k^2 + c_j t_k^2 + \epsilon_{ijk} \quad (\text{M2c})$$

$$Y_{ijk} = a + a_j + bt_k + b_j t_k + ct_k^2 + c_j t_k^2 + \epsilon_{ijk} \quad (\text{M3})$$

Model (M0) is the simplest: the expected log ratio Y_{ijk} is modeled by a straight line, the slope b of which does not depend on dilution. In model (M1), the slopes $b + b_j$ may depend on dilution. In the actual fit, the slopes are found to decrease as the initial proportion of RL increases. This is coherent with Figure 1. However, it hides the relevance of the quadratic models. Model (M3) is the complete log-quadratic model: both the slopes $b + b_j$ and the curvatures $c + c_j$ may depend on dilution. Models (M2b) and (M2c) are embedded into (M3): in model (M2b) the slope does not depend on dilution and in (M2c) the curvature does not depend on dilution.

For all four models, the linear fit was computed, then pairs of embedded models were tested by the Fisher test of analysis of variance. The results are presented in Table 3: the degrees of freedom df , the Fisher test statistic F , and the significance p -values are given. The conclusions are the following. The first three comparisons are significant, ie the bigger model is better than the embedded one. The (M3) vs. (M2c) comparison is not. The conclusion of the four comparisons is that the best fitted model is (M2c). This indicates that if curvatures are included in the model, the slopes do not significantly depend on dilution. This is coherent with the theoretical derivation of the log-quadratic model (7). In model (M2c) the estimated slope is $\hat{b} = 6.1 \times 10^{-3}$ and 95% confidence interval on b is $[5.6 \times 10^{-3}; 6.6 \times 10^{-3}]$. Recall from (7) that the slope b of (M2c) should be understood as the difference between the slopes of models (9) for RL and THP-1. From the two previous sections, the estimated difference is 1.01×10^{-2} , which is above the confidence interval on b in (M2c).

Next, we tested the three pairwise differences of curvatures c_j in the accepted model (M2c). The results are presented in Table 4: the value of the

Embedded models	df	F	p-value
(M3) vs. (M2b)	(2, 291)	24.67	1.3×10^{-10}
(M2b) vs. (M1)	(1, 293)	22.8	8×10^{-39}
(M1) vs. (M0)	(2, 294)	118	1.8×10^{-38}
(M3) vs. (M2c)	(2, 291)	2.68	0.0705

Table 3: Tests of embedded models for the log ratio of RL vs THP-1 cell counts.

null hypothesis	t	p-value
$c_1 = c_2$	2.4	0.016
$c_1 = c_3$	17.9	6.3×10^{-49}
$c_2 = c_3$	16.1	4.5×10^{-42}

Table 4: Pairwise tests for differences in curvatures c_j in model (M2c).

Student test statistic t , and the p -value are given (degrees of freedom: 293). All three differences are significant. The estimated values of the curvatures $c + c_j$'s are given in Table 5. It turns out that $c_1 > c_2 > c_3$. So the curvature $c + c_j$ decreases as the initial proportion of RL increases. This is a similar phenomenon as was observed on Figure (1). Indeed, when curvatures are neglected (model (M1)), the slopes were found to be decreasing as the initial proportion of RL increases. The theoretical explanation is given by the mathematical model. Model (M1) amounts to keeping only the first term in the Taylor expansion (5). Since the next term is positive, the adjusted values of the slopes increase with time. Model (M2c) considers the first two terms in (5), neglecting the third one. If that neglected term is positive, then the same effect will occur: adjusted values of curvatures increase with time. The third term is proportional to the skewness of B . Observing decreasing curvatures as in Table 5 is an indication that the skewness of B may be positive, where B is the (random) difference in growth rate between RL and THP-1. Koutsoumanis and Lianou⁵ have proposed a logistic distribution as a model for growth rate variability. That distribution has null skewness. We conjecture that distributions with positive skewness provide better models for variable growth rates.

Conclusion

That unchecked populations grow exponentially fast is a well known fact, backed up by countless experiments, which validate the mathematical theory

Dilution j	$c + c_j$
$j = 1$ (0.5%)	5.3×10^{-6}
$j = 2$ (1%)	4.96×10^{-6}
$j = 3$ (5%)	1.6×10^{-6}

Table 5: Estimated curvatures $c + c_j$ in model (M2c).

of branching processes.⁴ To any clone stemming from a single cell can be associated an *exponential growth rate*, also called Malthusian parameter. It can be seen as the slope over a large interval of time, of the line fitting logarithms of the number of cells against time. What is questioned here, is the idea that clones stemming from different cells in a given strain, should have the same growth rate. Unlike Koutsoumanis and Lianou⁵ or Tomelleri et al,¹¹ we do not provide direct evidence for the intrinsic variability of growth rates, but instead an indirect proof, coming from a simultaneous growth experiment.¹⁰

It consisted in growing in the same vessels two cancer cell lines, RL⁸ and THP-1.⁹ If there existed a single growth rate for all RL clones, and another for all THP-1 clones, then the ratio should grow exponentially, the rate being the difference of the two growth rates. In that case, the growth rate of the ratio should not depend on the initial proportion of RL vs. THP-1. Our observations disproved this: the growth rate of the ratio was found to increase as the initial proportion of RL decreased (Figure 1). Assuming that growth rates may vary among clones provides both intuitive, and theoretical explanations.

The intuitive explanation is the following. Consider a growth rate as attached to each cell of a given clone. If clones may grow at different rates, the proportion of cells in faster growing clones will gradually increase. In other words, the distribution of growth rates at increasing times will be shifted toward larger values. This explains why, when the initial proportion of RL cells is 0.5%, at the time it reaches 5%, the population of RL contains more fast breeders than at time 0. Therefore, the (apparent) growth rate for an initial proportion of 0.5% is larger than for an initial proportion of 5%.

The theoretical explanation is the following. If growth rates of different clones are considered as independent random variables with a positive variance, then the model fitting the logarithms of cell numbers against time must contain a quadratic term, proportional to the variance of growth rates: variable growth rates imply that higher order terms must be added to the classical log-linear model. Now if a population grows according to a log-quadratic model,

and a log-linear model is fitted instead, then the estimated slope over an interval of time should increase as the interval moves to the right (see Figure 2). This will overestimate the mean growth rate.

To validate our theoretical explanation, we had to compare the fits of the log-linear and log-quadratic models on our experimental data. On separate growth data, the log-linear model was better than the log-quadratic model on RL, the contrary was true for THP-1. On simultaneous growth data, the log-quadratic clearly provided a better fit. This may seem paradoxical: indeed, the same model should be adopted for separate and simultaneous growths. The explanation of this apparent contradiction is statistical. The estimated curvature terms are in all cases smaller by several orders of magnitude than the estimated slopes. Therefore, the log-linear and log-quadratic models can hardly be distinguished when the cell counts range over several orders of magnitude, as in separate growths. This cannot be the case on simultaneous growth data, where the ratios range from a few percents to 100%. We believe that, on a separate growth experiment, if more values were collected at the beginning, then the log-quadratic model would provide a better fit.

There remains the issue of a probabilistic model to be fit on variable growth rates. Our derivation of the cumulant generating function shows that classical models of positive random variables, such as Gamma, Log-normal, or Logistic distributions⁵ cannot be used here. Indeed their exponentially decaying tail implies that the *equivalent growth rate* would become infinite at finite time, which is not realistic. So a truncated model would have to be used instead. In any case, there would remain to adjust the chosen distribution to actual data. Ideally, these data should be collected from the observation of colonial growth of individual cells, such as reported by Koutsoumanis and Lianou for *Salmonella enterica*,⁵ or Tomelleri et al¹¹ on leukemia cells. This will be the object of future work.

Acknowledgements

This work was supported by Laboratoire d'Excellence TOUCAN (Toulouse cancer). The authors are indebted to the anonymous referees for important suggestions.

Disclosure

The authors report no conflicts of interest in this work.

References

- ¹ L. M. Chevin. On measuring selection in experimental evolution. *Biol. Letters*, 7(2):210–213, 2011.
- ² F. Manna, R. Galet, G. Martin, and T. Lenormand. The high-throughput yeast deletion fitness data and the theories of dominance. *J. Evolutionary Biol.*, 25(5):892–903, 2012.
- ³ E. O. Powell. Growth rate and generation time of bacteria with special reference to continuous culture. *J. General Microbiol.*, 15(3):492–511, 1956.
- ⁴ M. Kimmel and D. Axelrod. *Branching processes in Biology*. Springer-Verlag, New York, 2002.
- ⁵ K. P. Koutsoumanis and A. Lianou. Stochasticity in colonial growth dynamics of individual bacterial cells. *Appl. Environ. Microbiol.*, 79(7):2294–2301, 2013.
- ⁶ E. K. Deenick, A. V. Gett, and P. D. Hodgkin. Stochastic model of T-cell proliferation: a calculus revealing IL-2 regulation of precursor frequencies, cell cycle time, and survival. *J. Immunology*, 170:4963–4972, 2003.
- ⁷ A. Zilman, V. V. Ganusov, and A. S. Perelson. Stochastic models of lymphocyte proliferation and death. *PLoS one*, 5(9):e12775, 2010.
- ⁸ M. Beckwith, D. L. Longo, C. D. O’Connell, C. Moratz, and W. J. Urbá. Phorbol ester-induced, cell-cycle-specific, growth inhibition of human b-lymphoma cell lines. *J. Nat. Cancer Institute*, 82(6):501–509, 1990.
- ⁹ S. Tsuchiya, M. Yamabe, Y. Yamaguchi, Y. Kobayashi, T. Konno, and K. Tada. Establishment and characterization of a human acute monocytic leukemia cell line (THP-1). *Int. J. Cancer*, 26(2):171–176, 1980.
- ¹⁰ D. E. Dykhuizen. Experimental studies of natural selection in bacteria. *Annu. Rev. Ecol. Syst.*, 21:373–398, 1990.

- ¹¹ C. Tomelleri, E. Milotti, C. Dalla Pellegrina, O. Perbellini, A. Del Fabbro, M. T. Scupoli, and R. Chignola. A quantitative study of growth variability of tumour cell clones in vitro. *Cell Proliferation*, 41(1):177–191, 2008.
- ¹² A. Novick. Growth of bacteria. *Annual Review of Microbiology*, 9:97–110, 1955.
- ¹³ M. H. Zwietering, I. Jongenburger, F. M. Rombouts, and K. van 't Riet. Modeling of the bacterial growth curve. *Appl. Environ. Microbiol.*, 56(6):1875–1881, 1990.
- ¹⁴ M. Peleg and M. G. Corradini. Microbial growth curves: what the models tell us and what they cannot. *Crit. Rev. Food Sci. Nutr.*, 51(10):917–945, 2011.
- ¹⁵ R. F. Brook. Variability in the cell cycle and control of proliferation. In P. C. John, editor, *The cell cycle*, pages 35–62. Cambridge University Press, 1981.
- ¹⁶ M.-L. Delignette-Muller. Relation between the generation time and the lag time of bacterial growth kinetics. *International journal of food microbiology*, 43(1):97–104, 1998.
- ¹⁷ F. Baty and M.-L. Delignette-Muller. Estimating the bacterial lag time: which model, which precision? *International Journal of Food Microbiology*, 91(3):261–277, 2004.
- ¹⁸ T. F. Hansen. Selection in asexual populations - an extension of the fundamental theorem. *J. Theor. Biol.*, 155(4):537–544, 1992.
- ¹⁹ T.E. Harris. *The theory of branching processes*. Springer-Verlag, Berlin, 1963.
- ²⁰ K. B. Athreya and P. E. Ney. *Branching processes*. Springer-Verlag, Berlin, 1972.
- ²¹ P. Mair. *Interpreting standard and non standard log-linear models*. Waxmann, Münster, 2006.
- ²² A. von Eye and E. Y. Mun. *Log-linear modeling: concepts interpretation, and application*. Wiley, New York, 2013.
- ²³ M. G. Kendall and A. Stuart. *The advanced theory of statistics: distribution theory*. Wiley-Blackwell, New York, 6th edition, 1994.

- ²⁴ A. Dembo and O. Zeitouni. *Large deviations techniques and applications*. Springer, New York, 2nd edition, 1998.
- ²⁵ G. Stone, B. Chapman, and D. Lovell. Development of a log-quadratic model to describe microbial inactivation, illustrated by thermal inactivation of *Clostridium botulinum*. *App. Environ. Microbiol.*, 75(22):6998–7005, 2009.
- ²⁶ S. Tsuchiya, N. Minegishi, M. Minegishi, T. Sato, and T. Konno. Adaptation of a human monocytic leukemia cell line (THP-1) in a protein-free chemically defined medium. *Tohoku. J. Exp. Med*, 150(4):455–465, 1986.